

Synchronization in Nanomechanical Oscillators

Anirban Ch Narayan Chowdhury

20081038

Abstract

Nanoelectromechanical systems incorporating nanomechanical elements find widespread potential applications in high-precision mass-sensing, noise filtering and many other areas. Arrays and networks of such oscillators can be used for pattern recognition and storing information. It is therefore of some interest to study the behaviour of coupled oscillators. Here we study synchronization in systems of two such oscillators coupled with and without delay. Complete synchronization, lag synchronization and anti-lag synchronization were obtained with coupled Duffing equations. Lag and complete synchronization were obtained using Duffing equation with cubic damping terms. Time-delayed coupling led to synchronization at weaker coupling strength.

Introduction

Nanoelectromechanical systems(NEMS) have been the subject of much research in recent years. These devices incorporate nano-scale mechanical oscillators. Other than increased energy efficiency, shrinking the mechanical component allows manufacture of devices with enhanced sensitivity and higher frequencies of operation. Such devices find potential application in mass-sensing, magnetic force resonance spectroscopy, noise squeezing.⁽¹⁾⁽²⁾⁽³⁾⁽⁹⁾ They can also be used as controllable memory elements.⁽⁸⁾

The experimental setup typically involves a doubly clamped beam with a periodic driving force provided by external electric or magnetic fields.^{(1),(2)(4)}

Doubly-clamped beam resonators are conveniently modelled by the forced Duffing equation⁽²⁾⁽⁴⁾:

$$m\ddot{x} + kx + ax^3 + b\dot{x} = f \cos(\omega t) \quad (1)$$

As can be seen, this equation is nonlinear in that it has a term proportional to the displacement-cubed. Nonlinear terms can arise due to external potentials or from the inherent geometry of the system, the latter being the case here.⁽⁴⁾

It has been found useful to add a nonlinear damping term proportional to the velocity-cubed. The physical effects contributing to damping in these devices are not clearly understood but it has been suggested that damping increases with increase in surface area, which is the case when dimensions are decreased.⁽¹⁾

The equation used is therefore of the form:

$$m\ddot{x} + kx + ax^3 + b\dot{x} + c\dot{x}^3 = f \cos(\omega t) \quad (2)$$

This is the equation that we have used in this study. It is to be noted however that this is equivalent to considering a damping term proportional to the velocity times the displacement squared.

For a wide range of frequency and amplitude of the driving force, these systems exhibit chaotic dynamics.⁽⁴⁾⁽⁵⁾ The time evolution of such a system is thus highly sensitive to initial conditions. Given a number of such oscillators, each will behave differently unless they are specified exactly identical initial conditions – which is impossible to realize in practice.

Coupling two or more such oscillators can lead to synchronization in their dynamics. In the simplest case, the two systems produce identical outputs and are said to be 'completely synchronized'. The systems may also show lag synchronization –the time series of the two are basically identical with a shift in time- and phase synchronization whereby the phase of the two systems become locked.⁽⁶⁾

Synchronization therefore allows control of chaotic dynamics. With a network of oscillators, synchronized states can be used for pattern recognition and possibly for storing information.⁽⁷⁾

In the following discussion we first look at the standard Duffing equation and then study how the behaviour changes with an additional cubic damping term. Then we consider two coupled Duffing oscillators and later introduce cubic damping in such a system. Finally, we study a system of two nanomechanical oscillators coupled with a time delay.

Dynamics of a Duffing Oscillator

Attractors and Bifurcations

The forced Duffing equation shows a wide variety of behaviour. It corresponds to a potential

$$V = \frac{kx^2}{2} + \frac{ax^4}{4}$$

This potential is single-welled if both k and a are positive and double-welled when k is negative but a is positive. We study a double-well oscillator with parameters $m=1$, $k=-1$, $a=1$, $b=.5$ in the Duffing equation -

$$m\ddot{x} + kx + ax^3 + b\dot{x} = f \cos(\omega t)$$

We varied the forcing amplitude f , starting from 0, and investigated the dynamics of the system.

To solve the system, first we rewrite the second-order differential equation as a system of three coupled equations in three variables x , y and z -

$$\dot{x} = y; \quad m\dot{y} = -kx - ax^3 - by + f \cos(z); \quad z = \omega t$$

Then we solve the system using the standard RK4 algorithm with a step-size of 0.1. Ignoring transients (approximately first 1000 iterations), phase portraits and time-series of x and y were plotted. From these we deduced the nature of the attractor, whether a point, periodic or chaotic.

The following table illustrates the route to chaos followed by the system with changing forcing amplitude

Forcing Amplitude	Nature of Orbit
$f = 0$	<i>Point attractor</i>
$f \leq 0.343$	<i>Closed orbit of period 1</i>
$0.344 \leq f \leq 0.355$	<i>Period 2 limit cycle</i>
$0.356 \leq f \leq 0.357$	<i>Period 4 limit cycle</i>
$0.358 \leq f \leq 0.365$	<i>Period doubling</i>
$0.366 \leq f \leq 0.383$	<i>One-band chaos</i>
$f > 0.383$	<i>Double-band chaos</i>

In the absence of forcing, the system settles into a point attractor on account of the damping. For small forcing, $f \leq 0.343$, we obtain a closed orbit or period 1. With increase in forcing amplitude, the system undergoes a bifurcation and we observe a period 2 limit cycle for $0.344 \leq f \leq 0.355$. The next bifurcation occurs at $f = 0.356$ and a period 4 limit cycle attractor is seen till

$f = 0.357$. Further period doubling is observed for $0.358 \leq f \leq 0.365$ and beyond that one-band chaos is observed, i.e., a chaotic attractor confined to one potential well. For $f > 0.383$ we get double-band chaos with a phase-space trajectory that crosses into both wells. Some of the phase-space trajectories have been shown in Fig. 1.

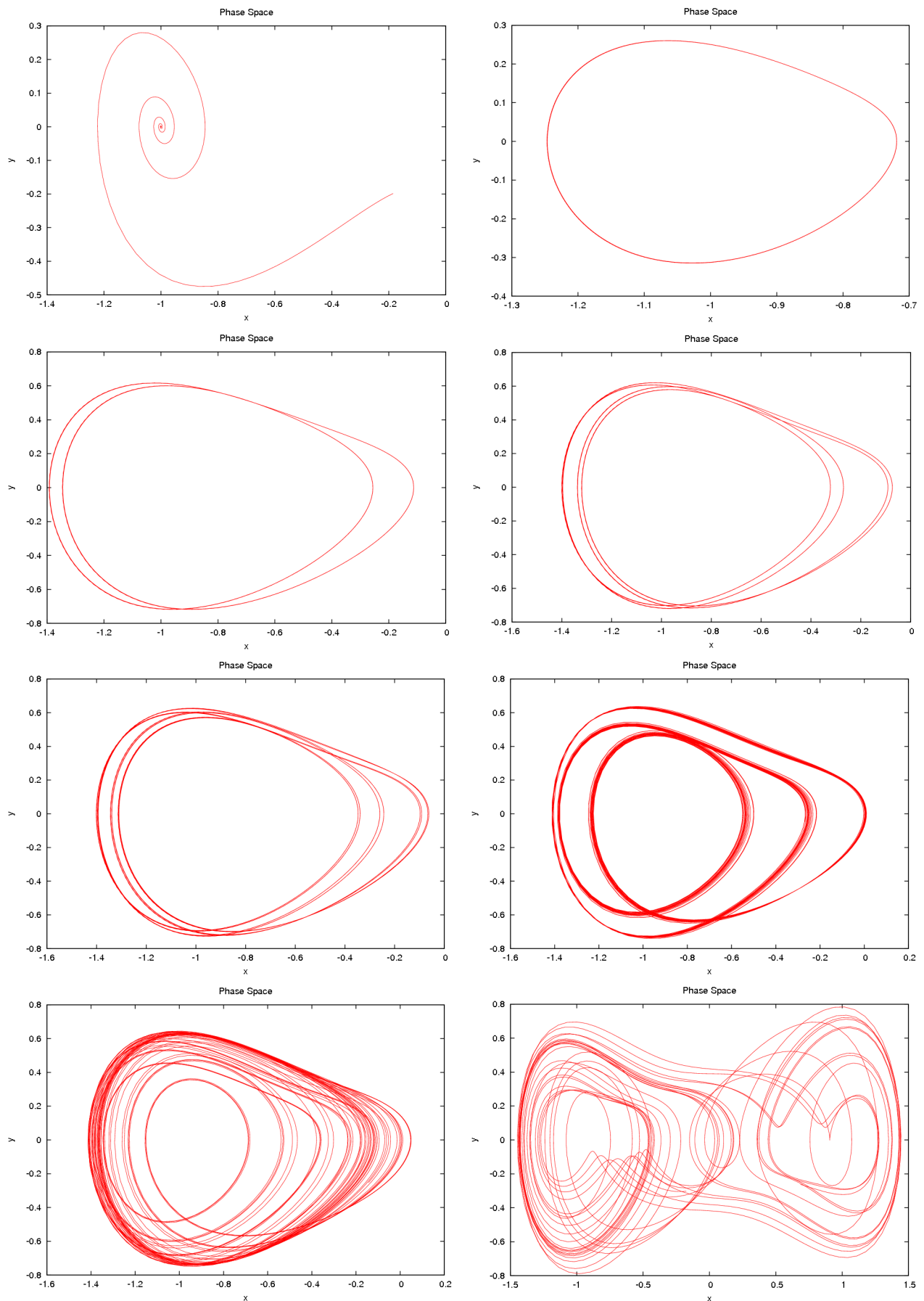


Fig. 1: Phase portraits of a double-well Duffing oscillator with parameters $m = 1$, $k = -1$, $a = 1$, $b = .5$ with forcing $0, 0.26, 0.349, 0.356, 0.358, 0.365, 0.37$ and 0.43

The route to chaos can be visualized more easily with the help of a bifurcation diagram. We tried to obtain one the following way:

- determine the time period of the period 1 limit cycle, say w iterations
- solve the system for 1000 f -values in the range $0.34 \leq f \leq 0.39$. to n iterations, say
- for each f ignore the first m iterations and then plot all x values at intervals of w , i.e., $x(i), x(i+w), x(i+2w), \dots, \text{etc.}$

With a step-size of 0.1, this scheme failed to work. We tried to determine the period by calculating the number of iterations between two maxima. The value returned was however either less or more than the actual period of the orbit because of the large step-size. Consequently, plotting the x -values at intervals of w gave us points scattered over wide ranges of x for limit cycles and chaotic attractors alike. Decreasing the step-size by a factor of 10 did not help much.

So we effected a change in the third step. We choose an interval slightly greater than w but strictly less than $2w$, say w_1 . Instead of plotting x at intervals of w , we plot the maximum of x over w_1 iterations, i.e., $\max[x(i), x(i+w_1)], \max[x(i+w_1), x(i+2w_1)], \dots, \text{etc.}$ A period 1 orbit will return a unique value, whereas a period 2 orbit will return 2 values, a period 4 will give 4 and so on.

With this method, we obtained the following bifurcation diagram which clearly shows a period-doubling route to chaos for the forced Duffing equation. Note that, for the bifurcation diagram, we used a step-size 0.01, deviating from the 0.1 used for the phase-portraits. A change in step-size did not lead to any appreciable change in the system's behaviour.

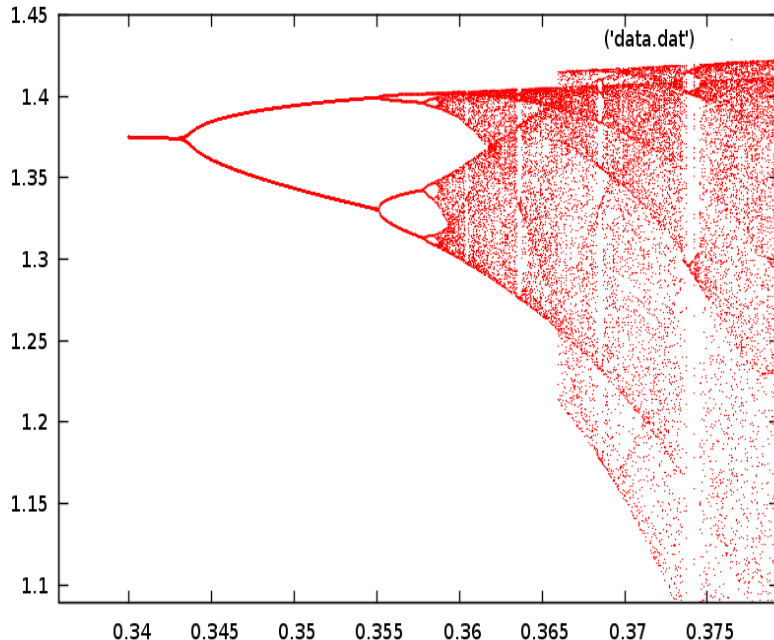


Fig.2: Bifurcation diagram of a Duffing oscillator with forcing amplitude

Basin Structure

As we have mentioned before, the Duffing oscillator is bi-stable and has two wells of attraction. With the given conditions, these wells are at $x=\pm 1$. For one-band chaos, the trajectories can end up in attractors in either well, depending on initial conditions. It is therefore instructive to plot the basin structure for the system.

We determined the basin structure for the region given by $-10 \leq x \leq 10$, $-10 \leq y \leq 10$. This was divided into a 100×100 rectangular grid, each point corresponding to a possible set of initial conditions for the system. For each point, the system was solved with parameters the same as before and a forcing amplitude $f=0.37$ (one-band chaos). The point was coloured red or blue depending on whether the chaotic attractor ended up in the well $x=-1$ or $x=1$ respectively.

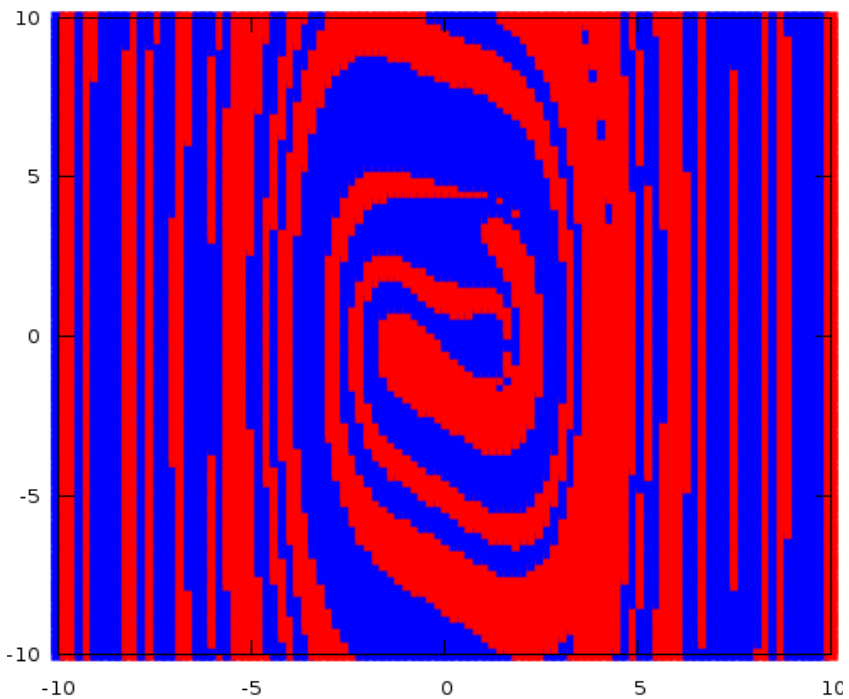


Fig. 3: Basin structure of Duffing oscillator: red and blue indicate chaotic attractors in two different wells, $x=-1$ and $x=1$ respectively

Dynamics of a Nanomechanical Oscillator

Attractors and Bifurcations

A similar analysis was performed for the Duffing equation with a small cubic damping term, $d=0.2$ in (2), keeping other parameters the same as that used for the standard Duffing equation.

The coupled equations are:

$$\dot{x} = y; m\dot{y} = -kx - ax^3 - by - dy^3 + f\cos(z); z = \omega t$$

As before, the system was solved for different values of f using the RK4 algorithm with a step-size of 0.1.

The following table illustrates the route to chaos.

Forcing Amplitude	Nature of Orbit
$f = 0$	<i>Point attractor</i>
$f \leq 0.382$	<i>Closed orbit of period 1</i>
$0.383 \leq f \leq 0.398$	<i>Period 2 limit cycle</i>
$0.399 \leq f \leq 0.402$	<i>Period 4 limit cycle</i>
$0.403 \leq f \leq 0.407$	<i>Period doubling</i>
$0.407 \leq f \leq 0.431$	<i>One-band chaos</i>
$0.432 \leq f \leq 0.436$	<i>Double-band chaos</i>
$f = 0.437$	<i>Limit cycle</i>
$f \geq 0.438$	<i>Double-band chaos</i>

The behaviour is not much different from the standard Duffing oscillator. Because of additional nonlinear damping,, higher forcing amplitudes are required to produce similar trajectories in phase-space for this 'nanomechanical oscillator'. For $f = 0$ we have a point attractor as before. We see a period 1 orbit for small forcing, i.e., $f \leq 0.382$. With further increase in forcing amplitude period doubling is observed and one-band chaos is seen for $0.407 \leq f \leq 0.431$. Even larger values of f lead to double-band chaos with a periodic window at $f = 0.437$.

Some of the possible trajectories are shown in Fig. 5.

A bifurcation diagram was constructed by the same method that we used for the Duffing oscillator (Fig. 4). It is similar to the one we obtained for Duffing. A period-doubling route to chaos can be clearly observed

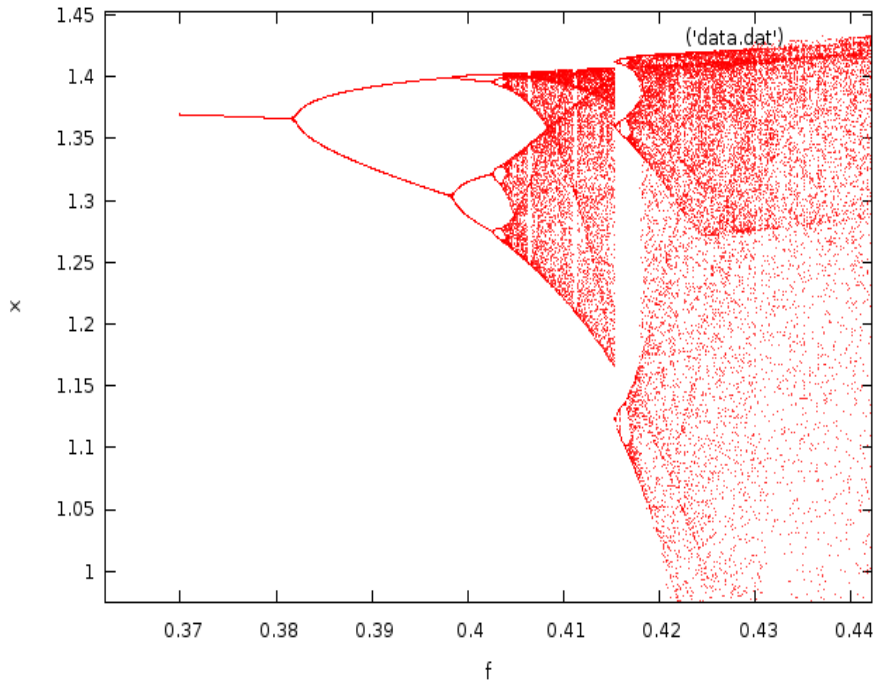


Fig. 4: Bifurcation diagram of a nanomechanical oscillator with forcing amplitude

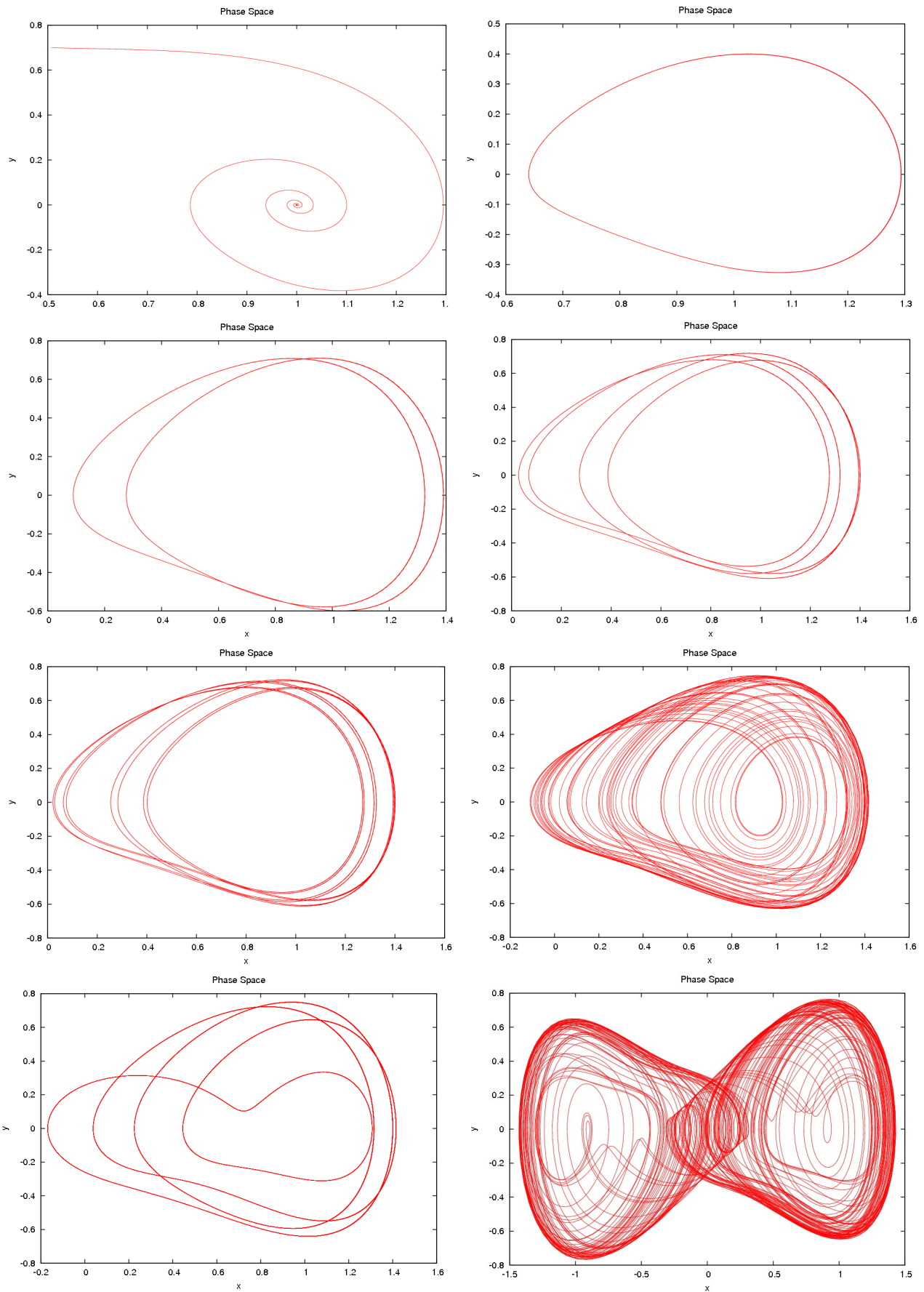


Fig. 5: Phase portraits of nanomechanical oscillator with parameters $m = 1$, $k = -1$, $a = 1$, $b = .5$, $c = 0.2$ with forcing 0, 0.3, 0.39, 0.402, 0.403, 0.42, 0.437 and 0.44 respectively

Basin Structure

The nanomechanical oscillator shows bi-stability similar to the forced Duffing oscillator. We have therefore two chaotic attractors in two different wells for one-band chaos. Following the same procedure as for Duffing, we obtain the basin structure. The basins of attraction here are well-separated, unlike in the case of Duffing.

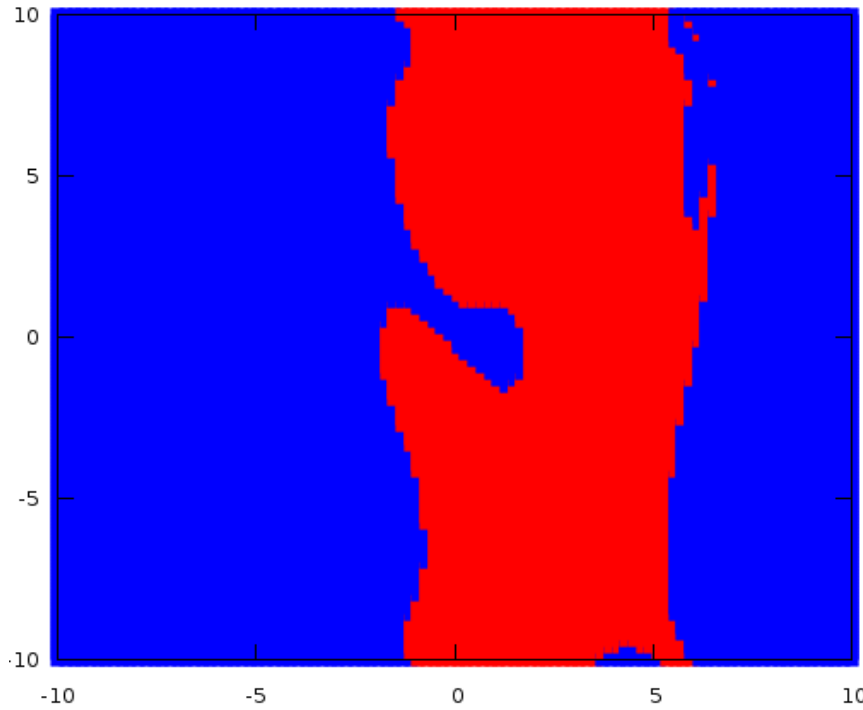


Fig. 6: Basin structure of nanomechanical oscillator; red and blue indicate chaotic attractors in two different wells, $x=-1$ and $x=1$ respectively

Dynamics of Two Coupled Duffing Oscillators

Route to Synchronization

In this section we investigate the route to synchronization of two coupled Duffing oscillators.

First let us write the Duffing equation as two coupled first order differential equations

$$\dot{x} = y ; \quad \dot{y} = -ay - bx - kx^3 + f\cos(wt)$$

The two oscillators are coupled by linear difference type coupling through the x -equation. The governing equations for two systems take the form:

$$\begin{aligned}\dot{x}_1 &= y_1 + c(x_2 - x_1); & \dot{y}_1 &= -ay_1 - bx_1 - kx_1^3 + f\cos(wt) \\ \dot{x}_2 &= y_2 + c(x_1 - x_2); & \dot{y}_2 &= -ay_2 - bx_2 - kx_2^3 + f\cos(wt)\end{aligned}$$

where c is the coupling coefficient.

We are interested in synchronization in the chaotic regime. Therefore, the forcing amplitude is set as such. For simplicity, we have considered only the case of one-band chaos with $f=0.37$

It turns out that for a particular coupling coefficient, the behaviour of the system is heavily dependent on the initial conditions in as much that the nature of the attractor (periodic/chaotic) was determined to some extent by the initial conditions.

To analyze the path to synchronization, we choose a set of initial conditions and vary the coupling constant.

Firstly, we have the following results with initial values

$$x_1(0)=1, y_1(0)=0, x_2(0)=0.5, y_2(0)=0$$

Coupling Coefficient	Behaviour
$0 \leq c \leq 0.027$	<i>Desynchronized chaos</i>
$0.028 \leq c \leq 0.29$	<i>Limit cycles of period > 2</i>
$0.03 \leq c \leq 0.045$	<i>Limit cycles of period 2, lag synchronization</i>
$0.045 \leq c \leq 0.057$	<i>Desynchronized chaos</i>
$c \geq 0.058$	<i>Complete Synchronization</i>

For a low coupling constant the two oscillators are desynchronized. With increase in the coupling strength, limit cycles are obtained. Period-halving is observed as the coupling strength is increased further till we obtain limit cycles of period 2. The limit cycles show lag synchronization. The two time series are identical with a time-shift. (Fig. 9) This time-shift – the 'lag' – was found to remain invariant at different values of the coupling coefficient. However, the system overall takes a longer time to settle into lag synchronization as c was gradually increased to 0.45.

In the range $0.045 \leq c \leq 0.057$ plots of synchronization errors - $x_1 - x_2$ and $y_1 - y_2$ show alternating highs and lows with time. (Fig. 10) The synchronization errors may tend to zero for a short period of time but the two oscillators are not synchronized in the long run.

Beyond .057 the trajectories of both oscillators are chaotic but they are completely synchronized. The synchronization errors go to zero in the asymptotic limit. (Fig. 11)

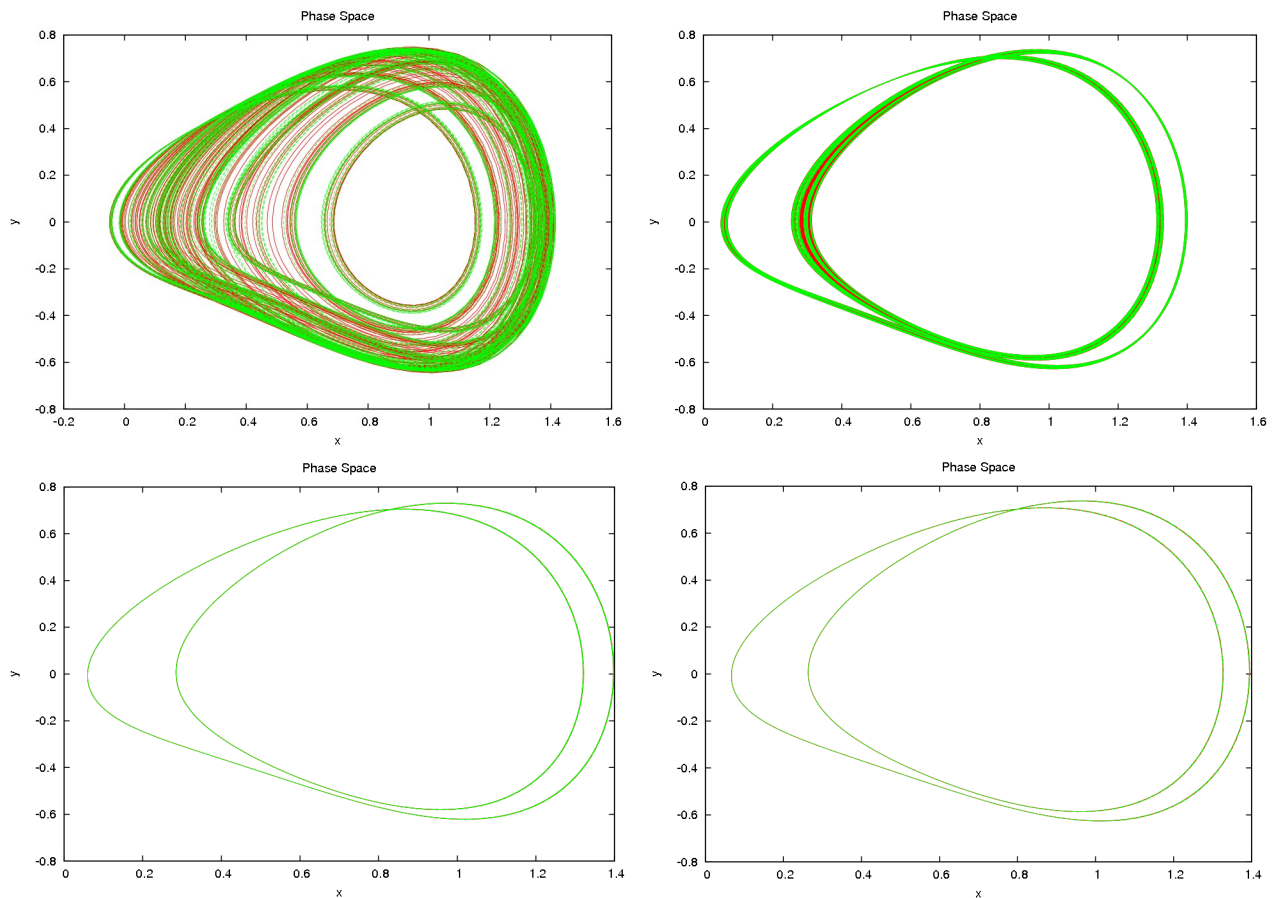


Fig. 7: Phase portraits of coupled Duffing oscillators with coupling strength 0, 0.028, 0.03, 0.039 respectively with identical initial conditions $x_1(0)=1, y_1(0)=0, x_2(0)=0.5, y_2(0)=0$

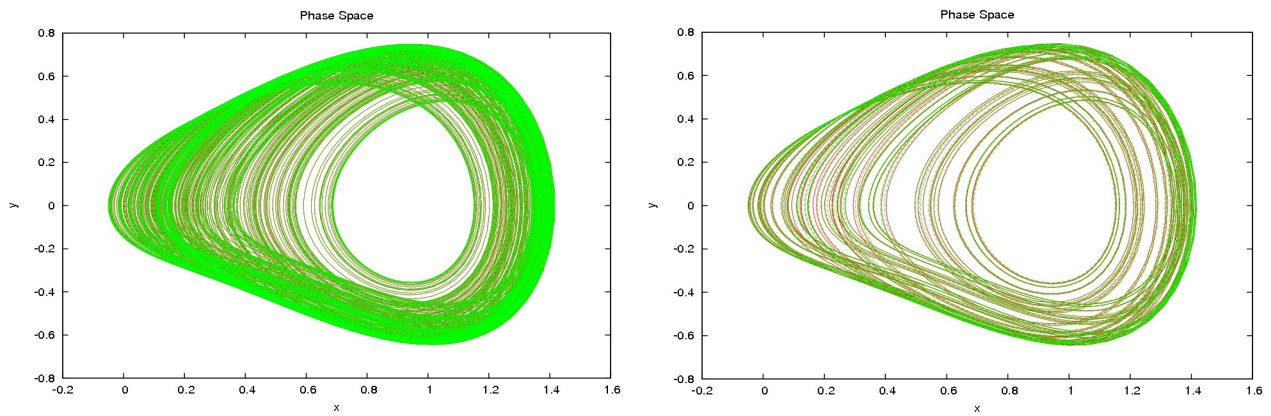


Fig. 8: Phase portraits of coupled Duffing oscillators with coupling coefficient 0.045 and 0.06 respectively with identical initial conditions $x_1(0)=1$, $y_1(0)=0$, $x_2(0)=0.5$, $y_2(0)=0$

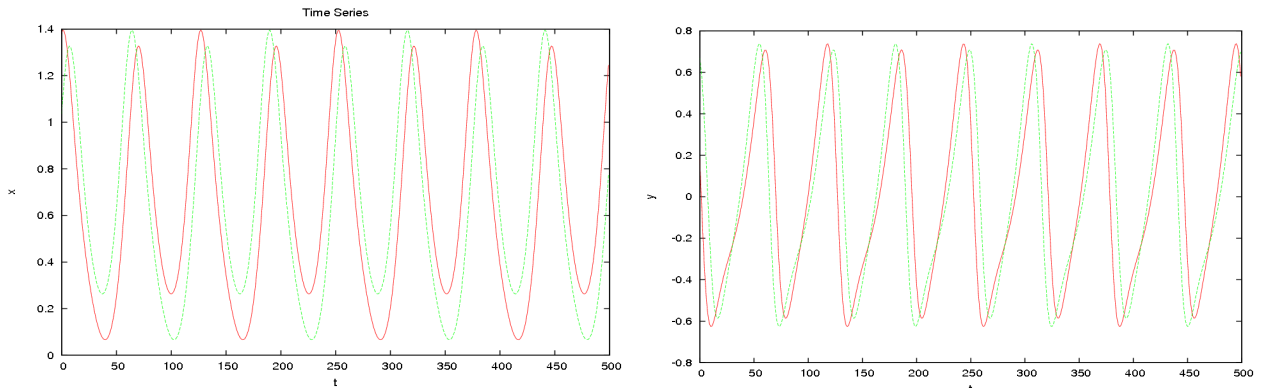


Fig. 9: Time series graphs of x and y for $c=0.039$

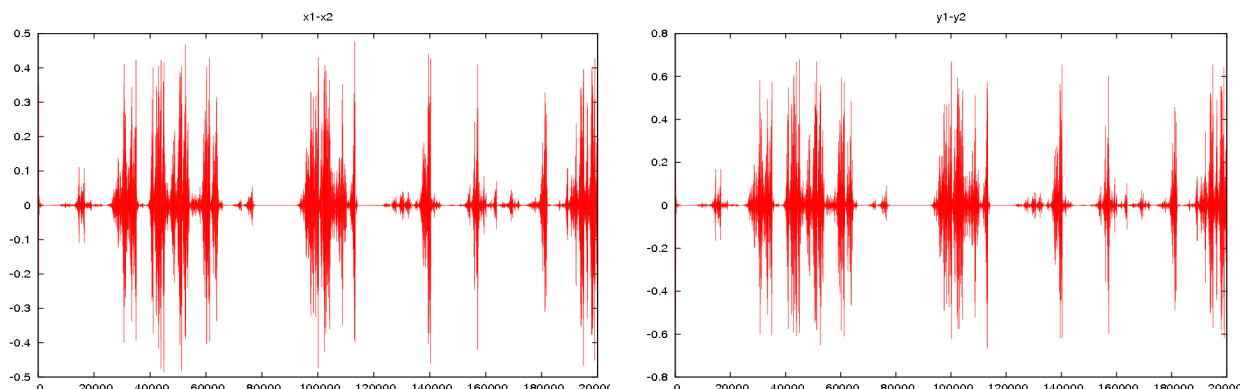


Fig. 10: Evolution of $\Delta x=x_1-x_2$ and $\Delta y=y_1-y_2$ over time for $c=0.055$

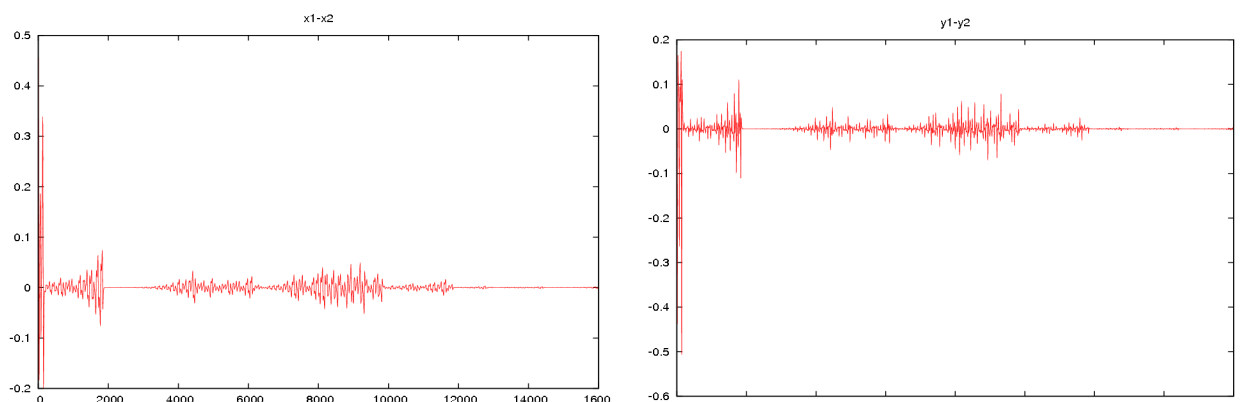


Fig. 11: Evolution of $\Delta x=x_1-x_2$ and $\Delta y=y_1-y_2$ over time for $c=0.059$

We now consider a different set of initial values

$x_1(0)=1.25$, $y_1(0)=0$, $x_2(0)=-1.25$, $y_2(0)=0$ The conditions are such that without coupling the two oscillators fall into two different chaotic attractors. The behaviour at different values of the coupling coefficient are tabulated below.

Coupling Coefficient	Behaviour
$0 \leq c \leq 0.076$	<i>Desynchronized chaos</i>
$0.077 \leq c \leq 0.091$	<i>Limit cycles of higher periods</i>
$0.092 \leq c \leq 0.0139$	<i>Limit cycles of low periodicity</i>
$0.0139 < c \leq 0.01425$	<i>Final state fluctuates between limit cycles and completely synchronized chaotic trajectories</i>
$c > 0.01425$	<i>Complete Synchronization</i>

A few of the phase-trajectories have been shown in Fig. 13. For weak coupling we have desynchronized chaotic attractors. With increase in coupling strength, limit cycles are observed and a period-halving is seen with increase in coupling strength.

The limit cycles show what may be called anti lag synchronization. The periodic attractors are in two different wells and the time series are essentially the mirror images of each other with a time-shift. (Fig.12) This behaviour is analogous to the previous case where we obtained lag synchronization in the same well. The time-lag in this case is also invariant at different values of the coupling coefficient.

However, in the previous case we observed a region of desynchronization between lag synchronization and complete synchronization. This is not observed here. Instead it is seen that within a certain range, as the coupling coefficient is increased, the system flips between anti-lag and complete synchronization alternately. Finally, after the coupling strength crosses a threshold, only complete synchronization is observed.

In the range $0.077 \leq c \leq 0.091$ the periodicity of the limit cycle changes. It was observed that the period decreases as c goes from .077 to .08. It increases again for $c=0.081$ but then onwards decreases again. (Fig. 14)

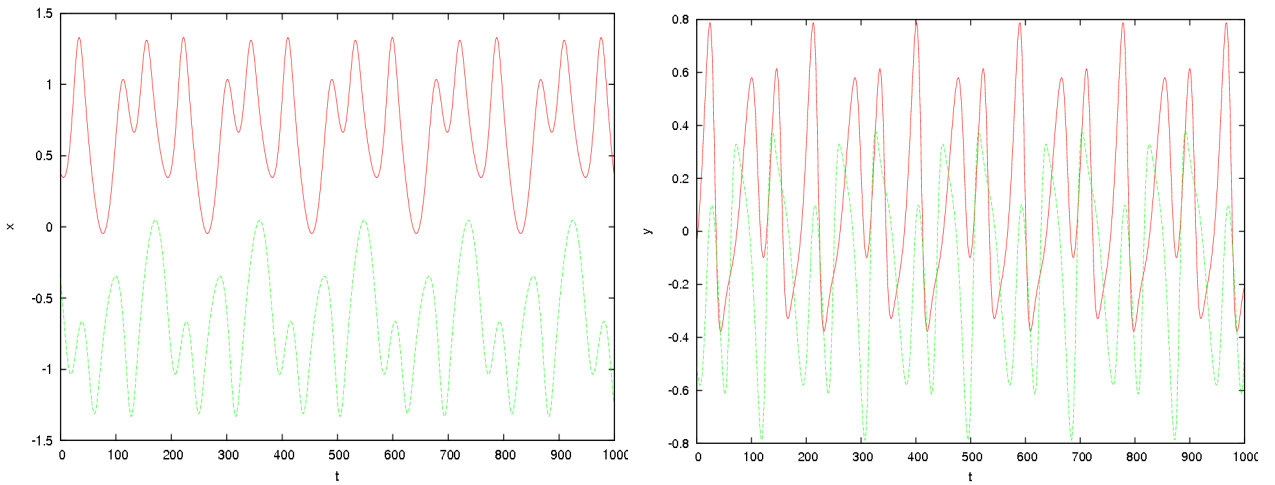
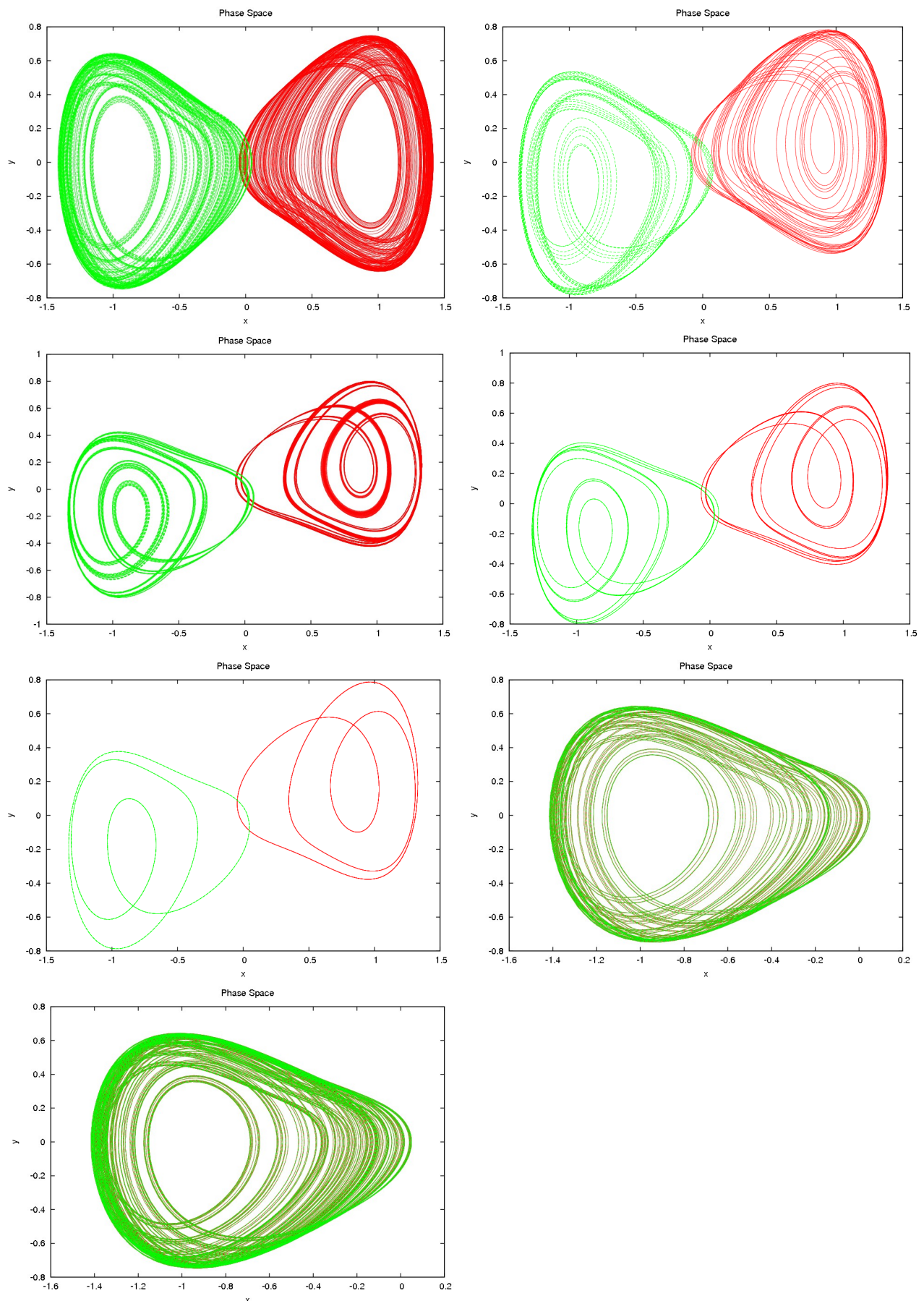


Fig. 12: Time-series of x and y for $c=0.093$



*Fig. 13: Phase-space portraits of coupled Duffing oscillators with coupling coefficient 0, 0.06, 0.08, 0.09, 0.093, 0.1395, 0.1399 respectively with identical initial conditions
 $x_1(0)=1.25$, $y_1(0)=0$, $x_2(0)=-1.25$, $y_2(0)=0$*

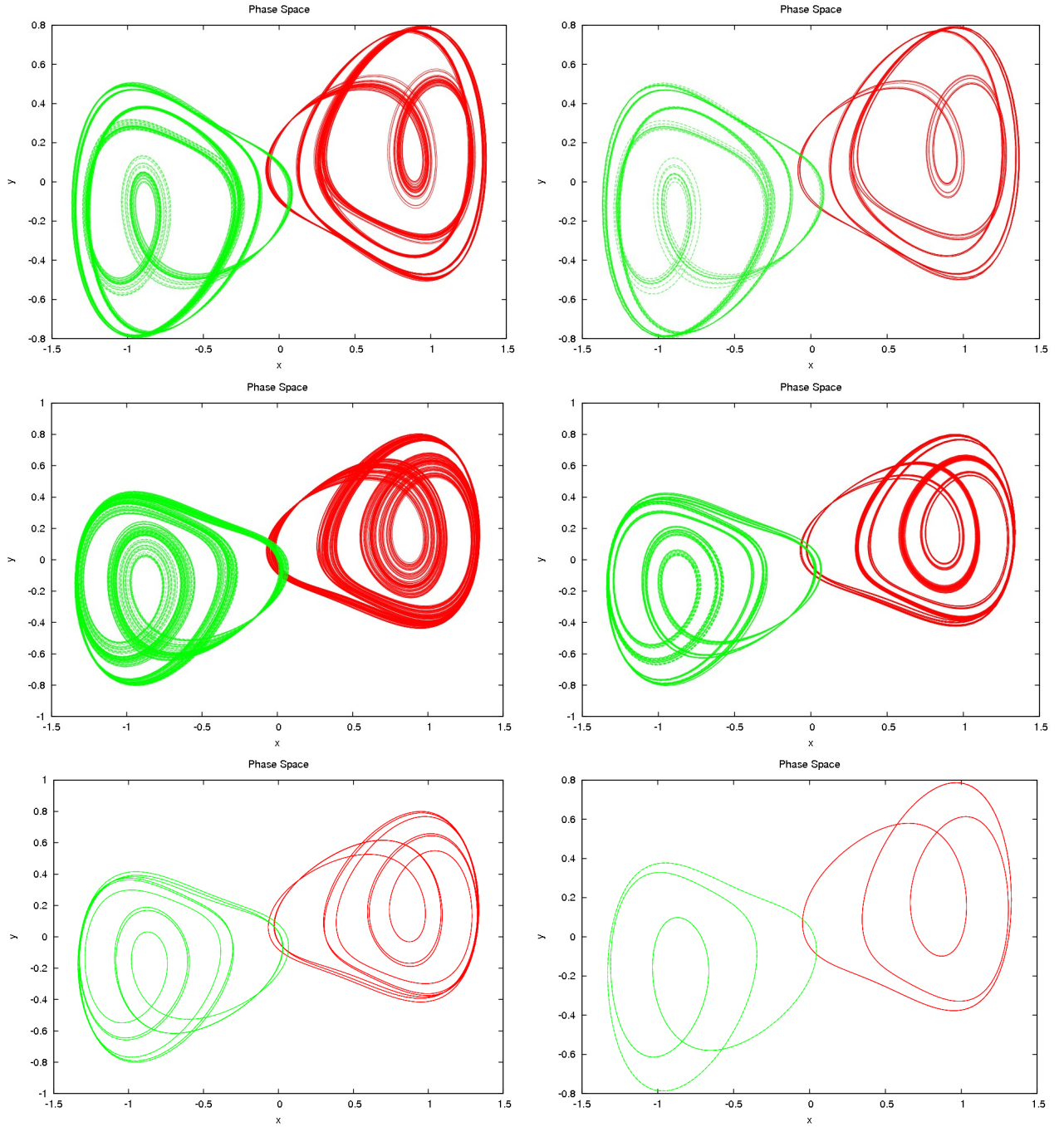


Fig. 14: Phase-space trajectories for $c=0.079, 0.08, 0.082, 0.085, 0.087$ and 0.093 ; period decreases from 0.079 to 0.08 but increases $.081$ and then onwards keeps decreasing till $c=.092$

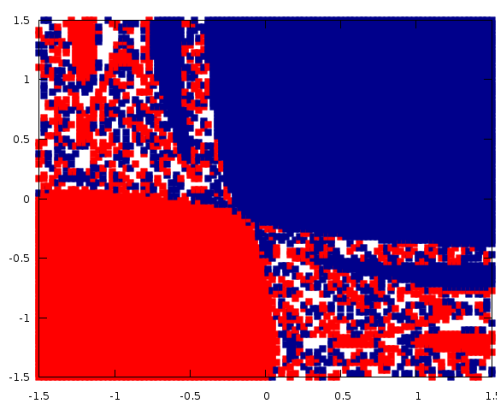
Similar analysis was performed with a few different initial conditions. The behaviour observed is similar to what we have already described.

Basin Structure

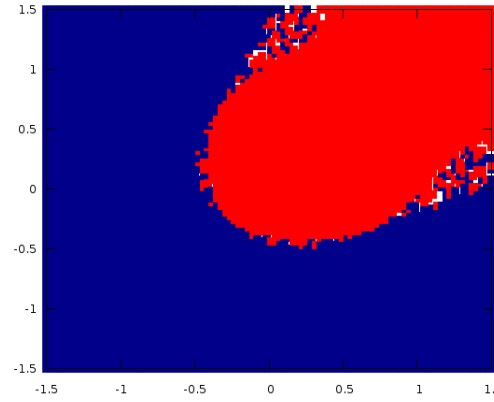
It was observed that at the same strength of coupling, the state of the system after sufficient time evolution depends on the initial conditions. It can vary between lag synchronization, anti-lag synchronization and complete synchronization, the last being in either well again dependent on initial conditions. This is a consequence of the bi-stable nature of the Duffing oscillator. Clearly it is helpful to obtain a complete basin structure for the system for a given coupling strength. The system has 4 degrees of freedom, so the entire basin structure cannot be visualized. We therefore plotted a

few 2-dimensional slices of the basin at a coupling strength of 0.15. The first three diagrams were plotted by keeping the initial y-values fixed and allowing the initial x-coordinates to vary between -1.5 and 1.5. The procedure used was identical to the one we used to obtain basin structures for one oscillator, the only difference being that here we have x_1, x_2 instead of x, y . The last one was obtained by varying the y-coordinates keeping the x-coordinates fixed. As can be seen from the figures, the basin structures show high degree of mixing in certain regions. An interesting observation is that anti-lag synchronization is obtained only for initial conditions corresponding to regions where the basin is highly mixed. In other regions lag synchronization is observed. This was verified by performing simulations with different sets of initial conditions. Therefore, depending on initial conditions, we see one of the two following routes to synchronization with increasing coupling strength -

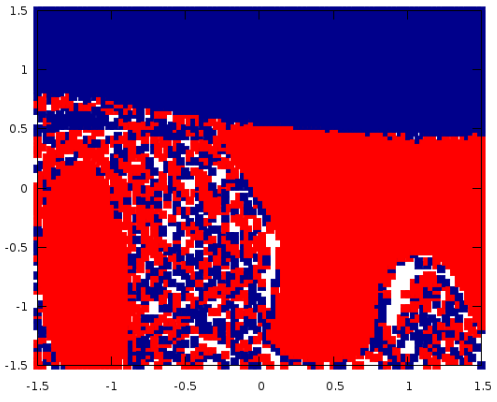
- 1) Desynchronized chaos, lag synchronized limit cycles, desynchronized chaos, completely synchronized chaos seen with initial conditions as seen with initial conditions
 $x_1(0)=1, y_1(0)=0, x_2(0)=0.5, y_2(0)=0$
- 2) Desynchronized chaos, anti-lag synchronized limit cycles, completely synchronized chaos as seen with initial conditions $x_1(0)=1.25, y_1(0)=0, x_2(0)=-1.25, y_2(0)=0$



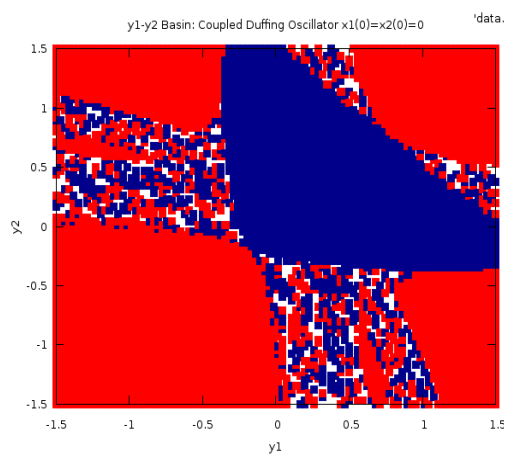
Basin 1: $y_1(0)=y_2(0)=0$



Basin 2: $y_1(0)=y_2(0)=1$



Basin 4: $y_1(0)=-y_2(0)=1$



Basin 3: $x_1(0)=x_2(0)=0$

Fig 15: Basin Structure of coupled Duffing oscillator in different planes: blue indicates complete synchronization in the well $x=1$, red in the well $x=-1$; white indicates absence of complete synchronization

Dynamics of Two Coupled Nanomechanical Oscillators

Route to Synchronization

We now repeat the same analysis for the nanomechanical oscillator equation, i.e., the Duffing equation with cubic damping. The parameters are kept the same as that used for a single oscillator and the forcing amplitude taken is 0.42, at which the oscillators show one-band chaos. The governing equations here are

$$\begin{aligned}\dot{x}_1 &= y_1 + c(x_2 - x_1); \quad \dot{y}_1 = -ay_1 - bx_1 - kx_1^3 - dy_1^3 + f\cos(\omega t) \\ \dot{x}_2 &= y_2 + c(x_1 - x_2); \quad \dot{y}_2 = -ay_2 - bx_2 - kx_2^3 - dy_2^3 + f\cos(\omega t)\end{aligned}$$

As in the case of Duffing, we choose initial values $x_1(0)=1, y_1(0)=0, x_2(0)=0.5, y_2(0)=0$

Coupling Coefficient	Behaviour
$0 \leq c \leq 0.026$	Desynchronized chaos
$0.027 \leq c \leq 0.031$	Limit cycles of higher periods
$0.032 \leq c \leq 0.045$	Limit cycles of period 2
$0.046 \leq c \leq 0.047$	Desynchronized, periods of high and low synchronization errors in time series
$c=0.048$	Limit cycle
$0.049 \leq c \leq 0.05$	Desynchronized, periods of high and low synchronization errors
$c \geq 0.051$	Completely synchronized

The behaviour is mostly the same as that obtained in the case of two coupled Duffing oscillators with the same initial values. For weak coupling, desynchronized chaotic attractors are seen.. With higher coupling strengths, limit cycles are observed. As before, we see period-halving with increase in coupling strength in the range $0.027 \leq c \leq 0.032$. The only different feature is the existence of a periodic attractor at $c=0.048$, whose nature is different from the limit cycles obtained at lower coupling strength. The limit cycles as before show lag synchronization, the two time series being identical with a constant time-shift (Fig. 16)

The system took a longer time to settle into synchronization – lag or complete - as the coupling coefficient tended to the region of desynchronized behaviour, i.e., close to the range

$0.046 \leq c \leq 0.05$ at say 0.045 or 0.051 (Figs. 18, 19)

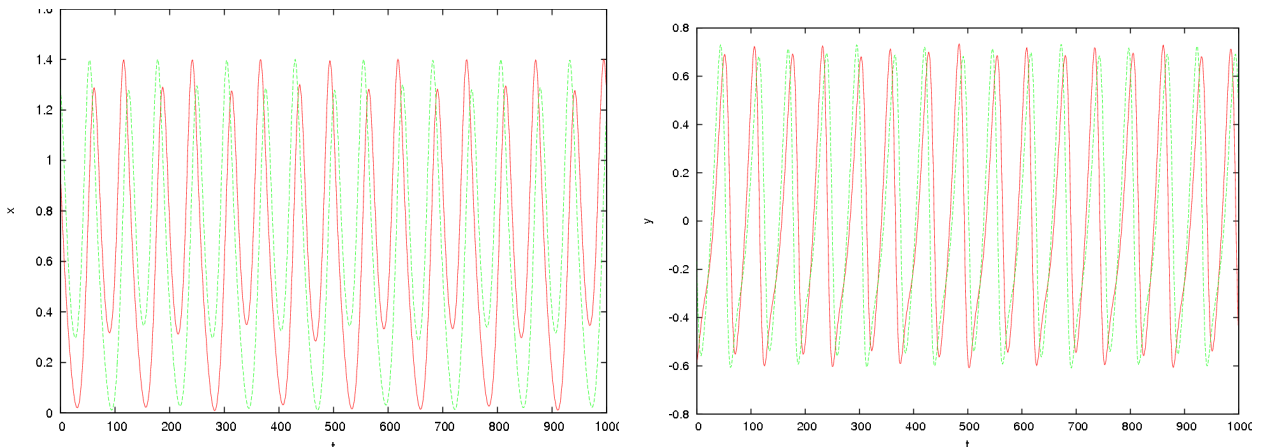
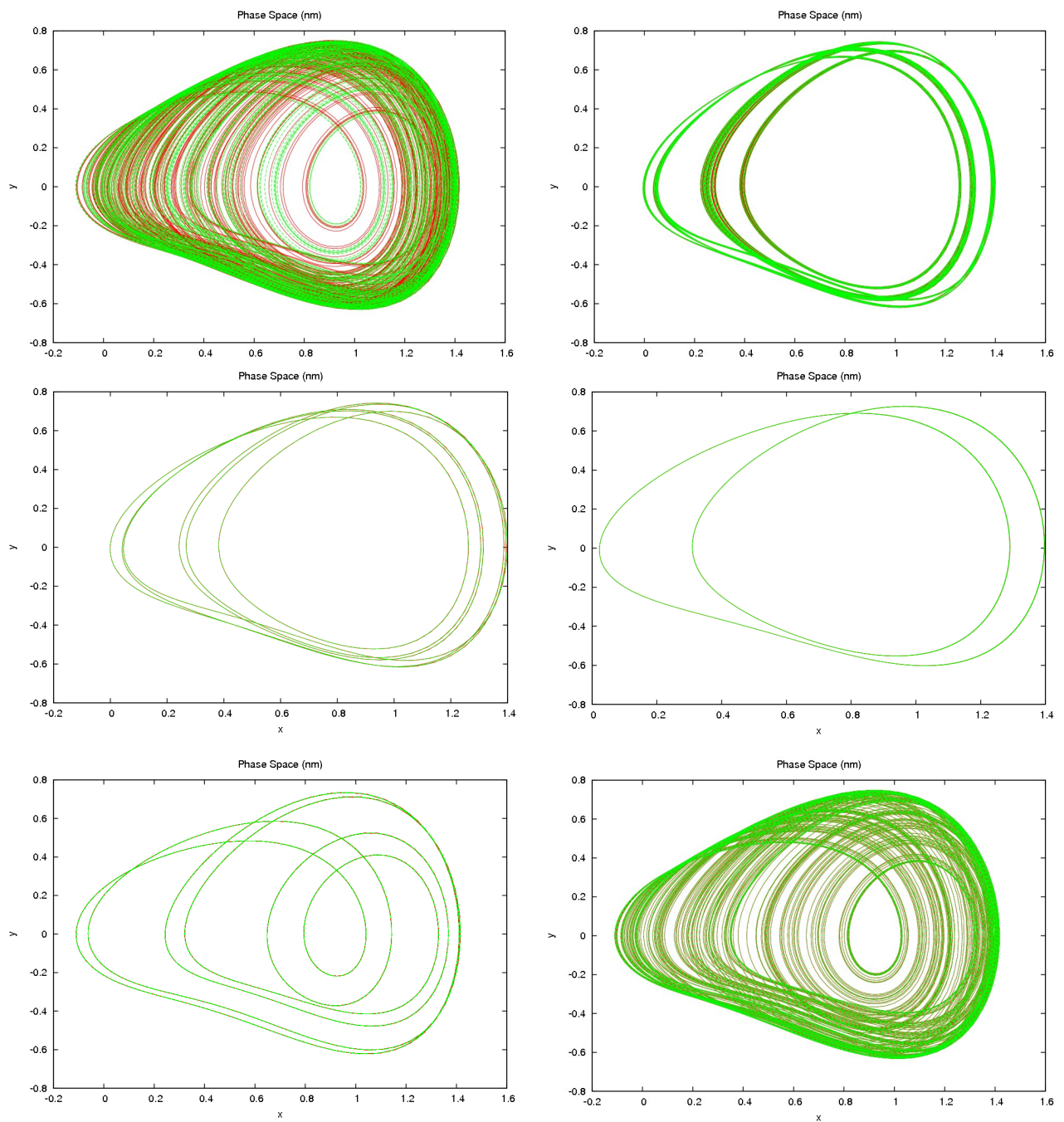


Fig. 16: Time series of x and y for $c=0.028$



*Fig. 17: Phase-space portraits for coupled nanomechanical oscillators with coupling coefficient 0.02, 0.03, 0.031, 0.032, 0.048 and 0.06 with identical initial conditions
 $x_1(0)=1$, $y_1(0)=0$, $x_2(0)=0.5$, $y_2(0)=0$*

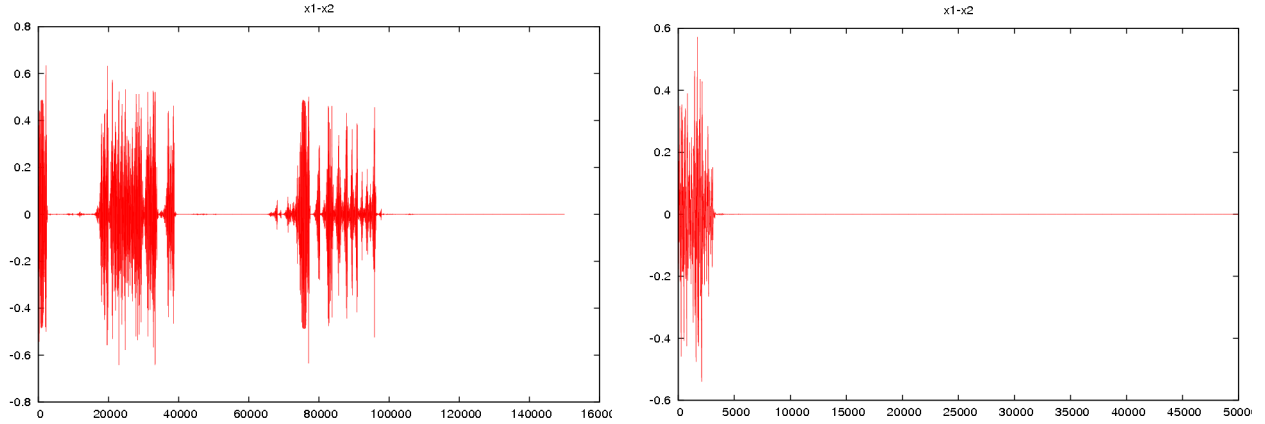


Fig. 18: Evolution of $\Delta x = x_1 - x_2$ over time for $c=0.051$ and $c=0.06$ respectively

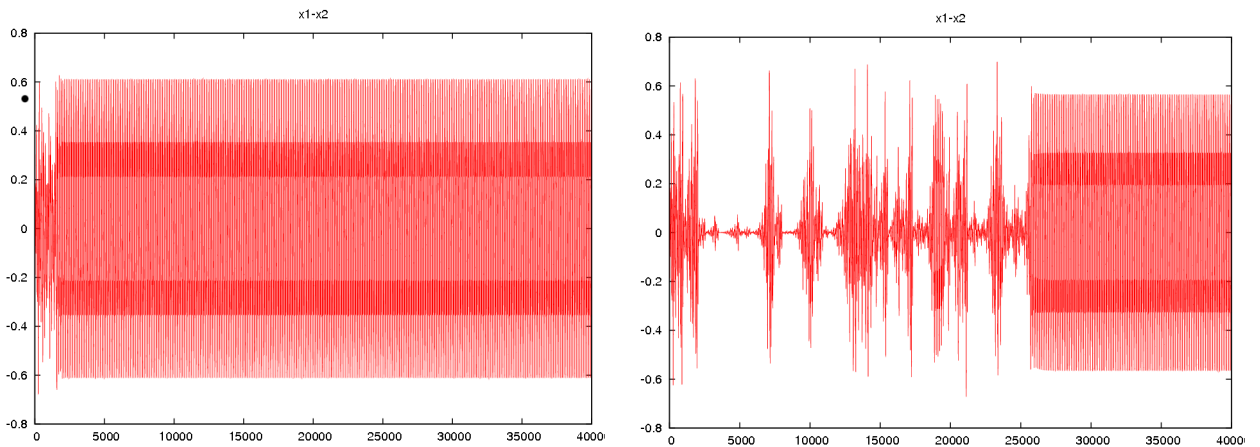


Fig. 19: Evolution of $\Delta x = x_1 - x_2$ over time for $c=0.038$ and $c=0.043$ respectively

Now, we consider a different set of initial values

$$x_1(0)=1.25, y_1(0)=0, x_2(0)=-1.25, y_2(0)=0$$

Coupling Coefficient	Behaviour
$0 \leq c \leq 0.036$	<i>Desynchronized chaos</i>
$0.037 \leq c \leq 0.044$	<i>Limit cycles of period 2</i>
$0.044 \leq c \leq 0.047$	<i>Desynchronized, periods of high and low synchronization errors in time series</i>
$c \geq 0.048$	<i>Complete synchronization</i>

There is a marked change in behaviour from the standard Duffing oscillator with identical initial conditions. Firstly, anti-lag synchronization is not observed with cubic damping. Limit cycles with lag synchronization are observed, but the two trajectories are in the same potential well. However, they can be either in the $x=1$ or $x=-1$ potential well, depending on the coupling strength. Well-flipping occurs for small changes in coupling strength. In this case, limit cycles of period >2 were not observed either.

Also, unlike the Duffing oscillator with the same initial conditions, here we have a range of c , where the oscillators are desynchronized, sandwiched between the lag synchronization and the complete synchronization ranges. This is however the same as what we observed for both Duffing and nanomechanical oscillators with initial conditions

$$x_1(0)=1, y_1(0)=0, x_2(0)=0.5, y_2(0)=0$$

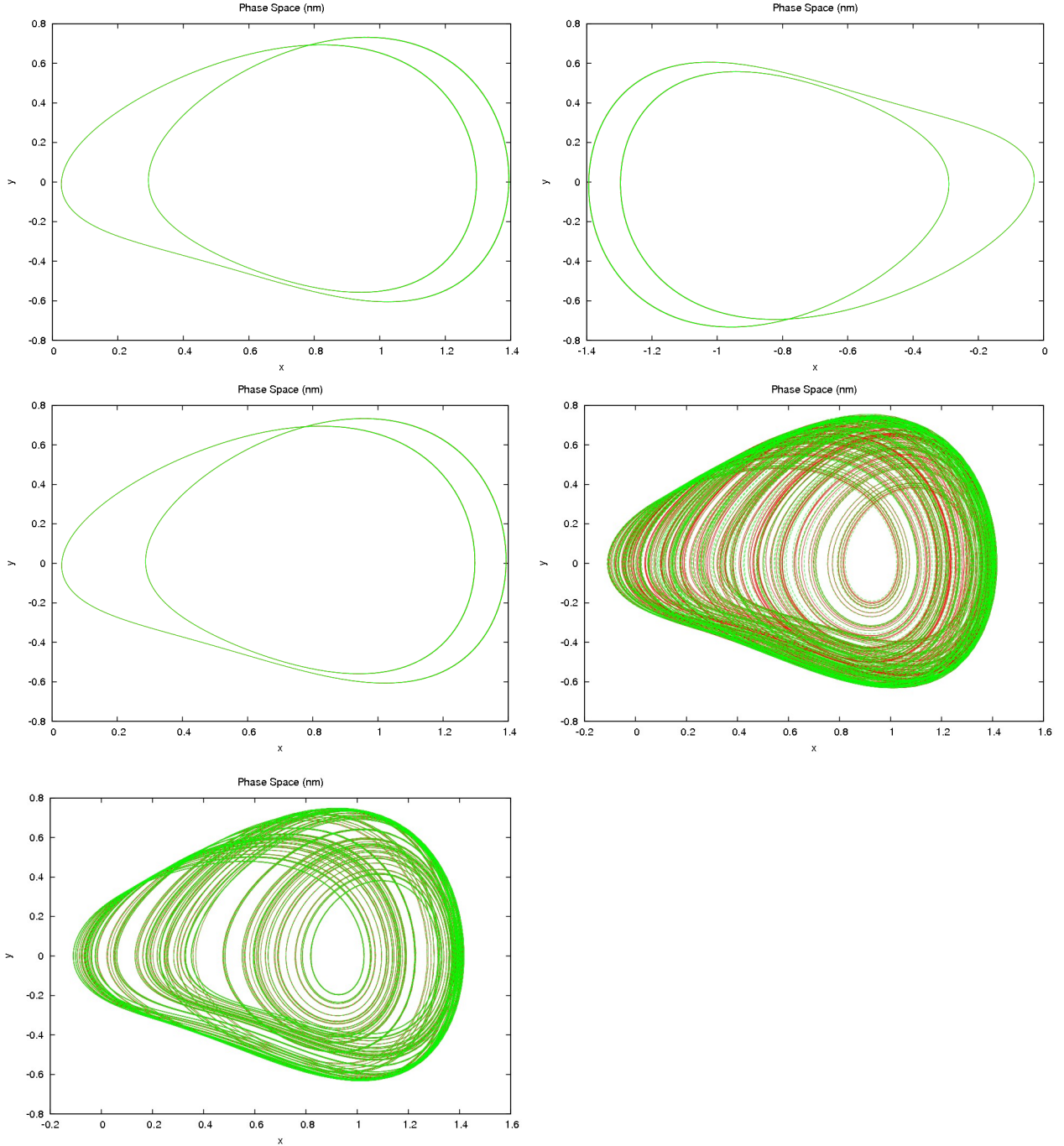


Fig. 20: Phase-space portraits of coupled nanomechanical oscillators with coupling coefficient 0.037, 0.038, 0.039, 0.044 and 0.06 respectively with identical initial conditions $x_1(0)=1.25$, $y_1(0)=0$, $x_2(0)=-1.25$, $y_2(0)=0$

Basin Structure

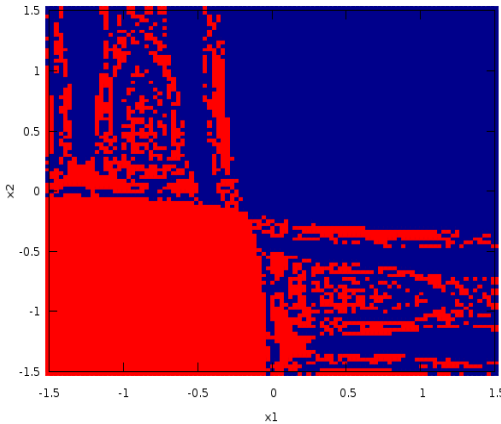
With different initial conditions, behaviour similar to the preceding two cases were observed. However, the coupling strengths determining the nature of the attractor and the state of synchronization changed with the initial values. This, as we have already mentioned, was also seen with two coupled Duffing oscillators. So, for this system too, we plotted sections of the basin in different planes with a coupling strength of 0.1. (Fig. 20) This ensured that the coupled system fell into complete synchronization after a short transient period. As can be seen, the basin structure is a lot similar to that for standard Duffing, with regions where the basins of attraction of the two

attractors are highly mixed.

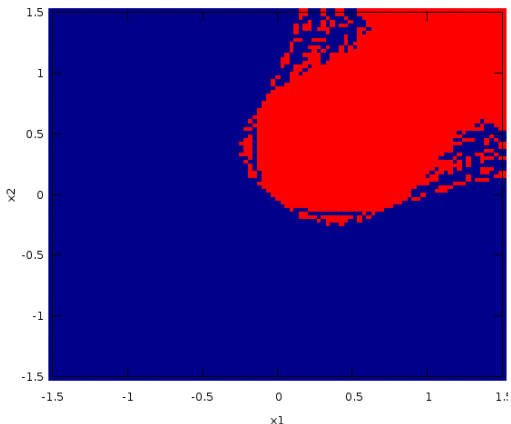
Our analysis with different initial conditions indicate that initial conditions given by points in the highly mixed regions show the same behaviour as

$$x_1(0)=1.25, y_1(0)=0, x_2(0)=-1.25, y_2(0)=0, \text{ while others show behaviour similar to } x_1(0)=1, y_1(0)=0, x_2(0)=0.5, y_2(0)=0$$

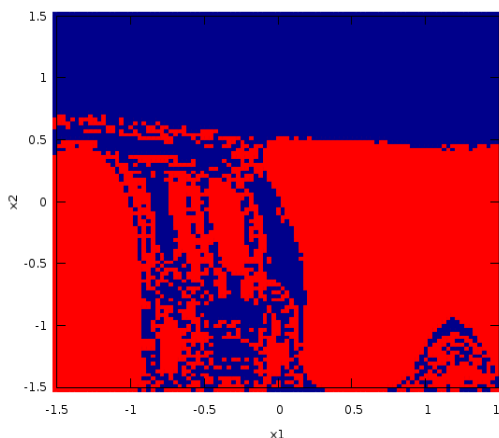
As in the case of two coupled Duffing oscillator , we see two routes to synchronization. But in this case, the routes are not as different/ primarily because anti lag synchronization is not observed for the nanomechanical oscillator.



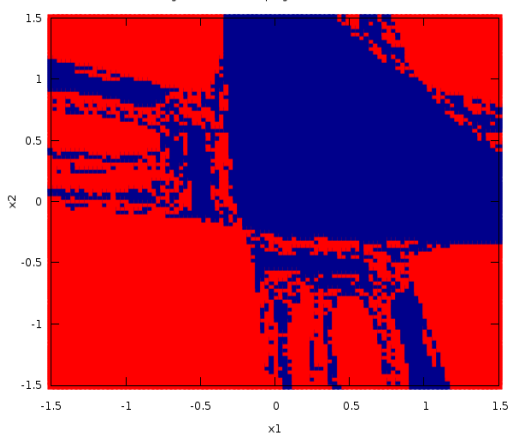
Basin 1: $y_1(0)=y_2(0)=0$



Basin 2: $y_1(0)=y_2(0)=1$



Basin 3: $y_1(0)=-y_2(0)=1$



Basin 1: $x_1(0)=x_2(0)=0$

Fig 21: Basin Structure of coupled nanomechanical oscillator in different planes: blue indicates complete synchronization in the well $x=1$, red in the well $x=-1$;

Dynamics of Two Nanomechanical Oscillators Coupled with a Delay

In actual systems of coupled oscillators, e.g., networks and lattices, time-delay in propagation of information from one oscillator to another needs to be accounted for. Therefore a delay needs to be introduced in the coupling term. In this section we examine such a model of two nanomechanical oscillators. The equations governing the dynamics are as follows:

$$\dot{x}_1(t) = y_1(t) + c(x_2(t-\tau) - x_1); \quad \dot{y}_1(t) = -ay_1(t) - bx_1(t) - kx_1(t)^3 - dy_1(t)^3 + f\cos(\omega t)$$

$$\dot{x}_2(t) = y_2(t) + c(x_1(t-\tau) - x_2(t)); \quad \dot{y}_2(t) = -ay_2(t) - bx_2(t) - kx_2(t)^3 - dy_2^3 + f\cos(\omega t)$$

τ denote the time delay. The simulations were run with initial conditions specified for both oscillators up to a time equal to τ . For the present case, the two oscillators were provided x-coordinates specified over [0.4,0.5] and [0.9,1] respectively. The initial y-coordinates were kept at zero. A weak coupling strength was chosen, $c=0.023$ such that the oscillators were not synchronized with zero time-delay.

Delay	Behaviour
$0 \leq \tau \leq 0.6$	<i>Desynchronized chaos; one oscillator shows one-band chaos while the other shows double-band chaos</i>
$0.7 \leq \tau \leq 0.9$.	<i>Desynchronized one-well chaos for both oscillators</i>
$1 \leq \tau \leq 1.7$	<i>Quasi-periodic trajectories, desynchronized</i>
$1.8 \leq \tau \leq 2$	<i>Different limit cycles, period decreases to 2 with increasing delay</i>
$2.1 \leq \tau \leq 3$	<i>Completely synchronized limit cycle or different limit cycles sensitive to initial conditions</i>
$3.1 \leq \tau \leq 3.6$	<i>Different limit cycles; period doubling</i>
$3.7 \leq \tau \leq 6.6$	<i>Desynchronized chaos; similar to $0 \leq \tau \leq 0.6$</i>
$\tau = 6.7$	<i>Different limit cycles</i>
$6.8 \leq \tau \leq 7.2$	<i>Completely synchronized limit cycle of period 2</i>
$\tau = 7.3$	<i>Different limit cycles same as $c=2$</i>
$7.4 \leq \tau \leq 8.2$	<i>Desynchronized chaos; same as $0 \leq \tau \leq 0.6$</i>

The corresponding phase-space diagrams can be seen in Figs 22 and 23.

A rich variety of behaviour is thus seen in the system. With small delay, the system is desynchronized, with one oscillator showing one-band chaos and the other showing cross-well chaos. As the delay is increased, both oscillators show one-band chaos and then desynchronized quasi-periodic trajectories. In the range $1.8 \leq \tau \leq 2$ the oscillators settle into two different limit cycles. A period-halving pattern is seen with increasing delay with a minimum period of 2. As we further increase the delay, we observe that in the range $2.1 \leq \tau \leq 3$ the final state of the system is sensitive to initial conditions. Starting with initial conditions randomly specified (within a small range) as we have, we either see a completely synchronized limit cycle state or a state with two oscillators in two different limit cycles; in both cases the cycles have period 2. In the range

$3.1 \leq \tau \leq 3.6$ we again see the oscillators falling into different limit cycles but here there is a period doubling with increase in delay. On increasing delay further, we get desynchronized chaotic attractors in $3.7 \leq \tau \leq 6.6$, similar to what was obtained with $0 \leq \tau \leq 0.6$. We see a periodic attractor at $\tau = 6.7$ but in the range $6.8 \leq \tau \leq 7.2$ completely synchronized limit cycles are

observed. Even more increase in delay drives the system to desynchronization again. This indicates that there may be a repeating pattern with changing delay.
A significant result is that complete synchronization of the oscillators has been achieved with a lower coupling strength than that required without delay.

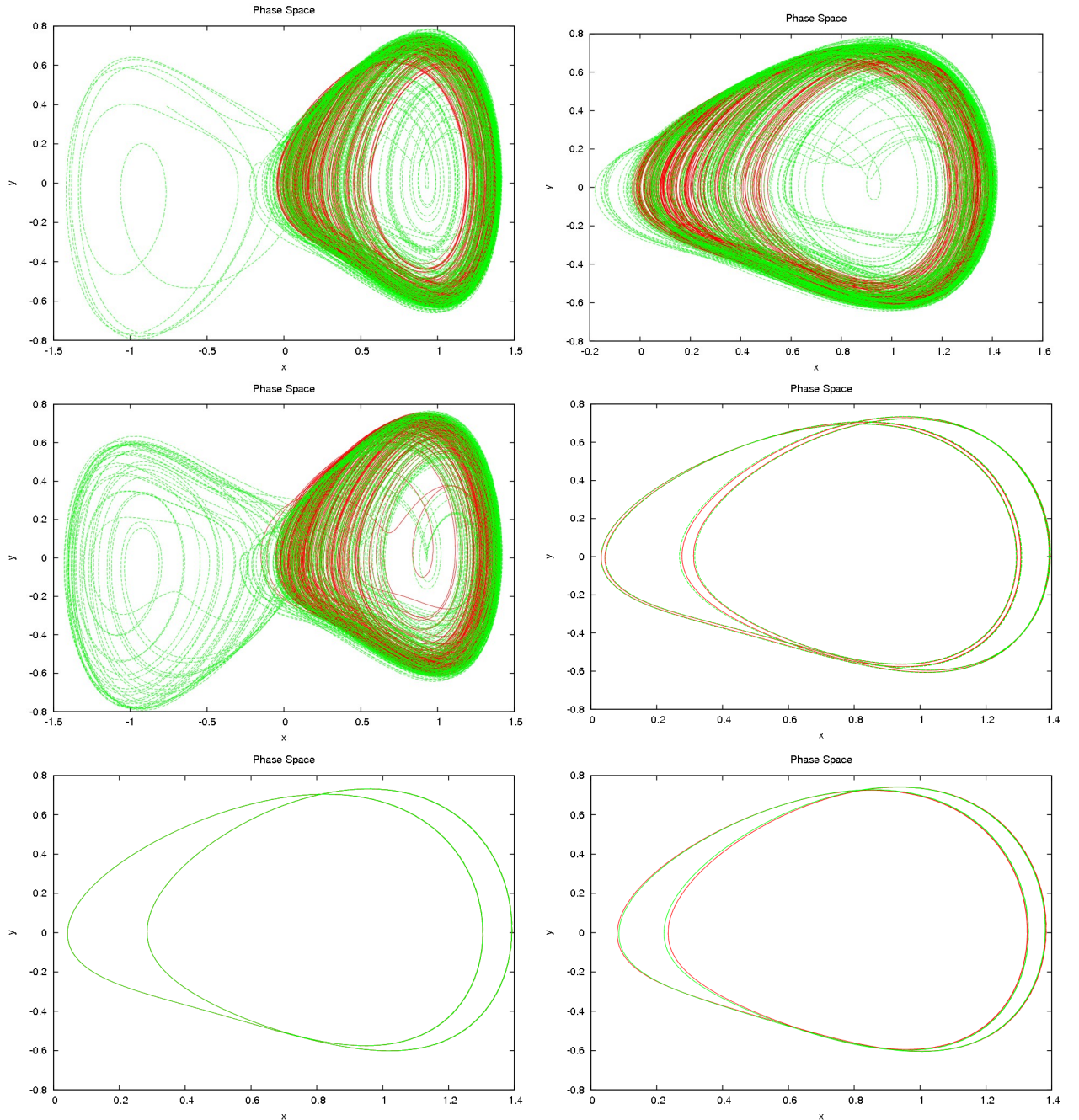


Fig. 22: Phase-space portraits for two nanomechanical oscillators coupled with delay at constant coupling, the delay being 0.5, 0.8, 4, 6.7, 6.8 and 7.3.

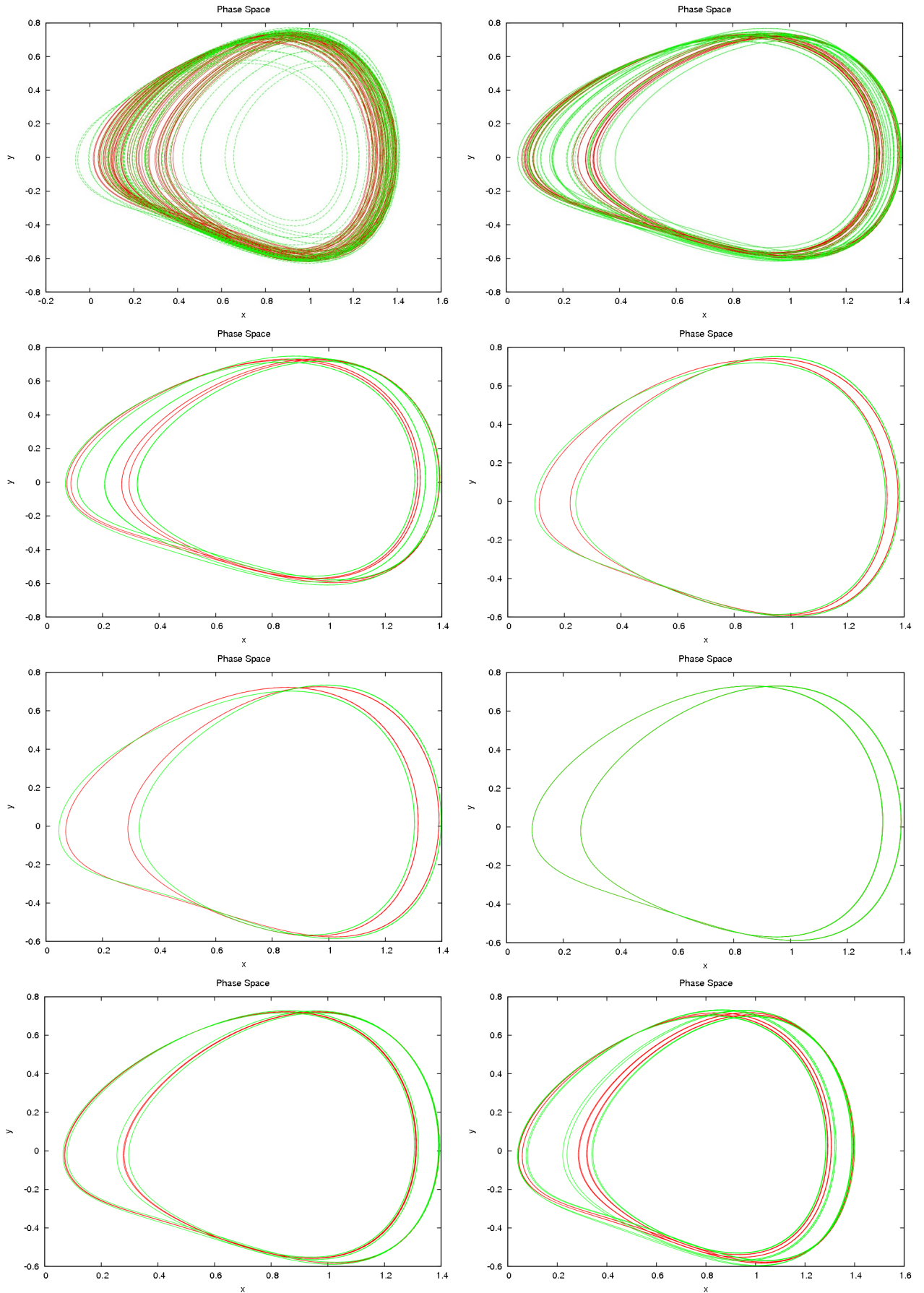


Fig. 23: Phase-space portraits for two nanomechanical oscillators coupled with delay at constant coupling, the delay being 1, 1.4, 1.8, 2, 2.5, 2.5 (with different initial values), 3.1 and 3.5

Conclusion

Let us now summarise the results we have obtained. First, we have observed that the nanomechanical oscillator equation shows dynamics qualitatively similar to the standard Duffing equation.

Then with a system of two coupled Duffing oscillators we have found that there exist two distinct routes to complete synchronization, depending on the initial conditions. In one case, as the coupling strength is increased, the system goes from desynchronized to lag synchronized state, followed by a period of desynchronization before finally settling into complete synchronization. In the other case, the system first goes into anti-lag synchronization, followed by a period of alternating anti-lag and complete synchronization, sensitive to small variations in the coupling strength. Finally the system settles into complete synchronization.

With coupled nanomechanical oscillators, the anti-lag synchronized state was not observed. Therefore with increasing coupling strength, the system followed similar routes to synchronization for different initial conditions. The completely synchronized states obtained in all these cases were chaotic.

Finally, in a system of two nanomechanical oscillators with delay-coupling, it was found that synchronization can be achieved at weaker coupling strengths by choosing suitable time-delays. In the case of delayed coupling however, the completely synchronized states were periodic.

The existence of synchronized states allows means of controlling the dynamics of systems of nanomechanical oscillators.

References

- (1) Nonlinear Damping in Nanomechanical Beam Oscillator - Stav Zaitsev, Student Member, IEEE, Ronen Almog, Oleg Shtempluck and Eyal Buks , Aug 2006 [<http://lanl.arxiv.org/abs/cond-mat/0406528v1>]
- (2) Noise-enabled Precision Measurements of a Duffing Nanomechanical Resonator - J. S. Aldridge and A. N. Cleland, June 2004
- (3) Nano-mechanical Oscillators Coupled to Optical Cavities – Ozan Aktas, May 2010
- (4) Nonlinear Dynamics of Nanomechanical and Micromechanical Resonators - Ron Lifshitz and M. C. Cross, March 2008
- (5) Nonlinear Dynamics: Integrability, Chaos and Patterns – Lakshmanan and Rajasekar, Springer, 2002
- (6) The Synchronization of Chaotic Systems - S. Boccalettia, J. Kurthsc, G. Osipovd, D.L. Valladaresb, C.S. Zhou, Physics Reports 366, 2002
- (7) Synchronized Oscillation in Coupled Nanomechanical Oscillators , Seung-Bo Shim, et al. Science 316, 2007
- (8) A Controllable Nanomechanical Memory Element - Robert L. Badzey, Guiti Zolfagharkhani, Alexei Gaidarzhy, Pritiraj Mohanty, Applied Physics Letters 85-16, October 2004
- (9) Noise Squeezing in a Nanomechanical Duffing Resonator - R. Almog, S. Zaitsev, O. Shtempluck, and E. Buks, Physical Review Letters 98-078103, February 2007

Acknowledgements

I would like to thank my mentor Dr. G. Ambika for her invaluable help and guidance.